Structure and Surface Properties of Plasma Polymerized Acrylic Acid Layers

DONG L. CHO,*[†] PER M. CLAESSON,[†‡] CARL-GUSTAF GÖLANDER,[†] and KENTH JOHANSSON,[†] [†]*The Institute for Surface Chemistry, Box 5607, S-114 86 Stockholm, Sweden; and* [‡]*The Surface Force Group, The Department of Physical Chemistry, The Royal Institute of Technology, S-100 44 Stockholm, Sweden*

Synopsis

Thin plasma polymerized layers of acrylic acid (PPAA) were deposited onto polyethylene and muscovite mica surfaces. Structure and surface properties of the deposited layer depend on the polymerization conditions. The content of carboxylic groups in the layer decreases, whereas the degree of crosslinking or branching increases, with increasing discharge power. A soft, sticky layer with a low contact angle against water is obtained when a low discharge power (5 W) is used. In contrast, a hard film with a rather high water contact angle is obtained when the discharge power is high (50 W). A surface force apparatus was employed to study some film properties including adhesion force, crack formation, and capillary condensation. The adhesion force between plasma polymerized acrylic acid layers prepared at a low discharge power is high in dry air. It decreases remarkably in humid air and no adhesion is observed in water. In dry air, the adhesion force between PPAA layers decreases as the discharge power increases.

INTRODUCTION

It is well established that interfacial phenomena such as wetting and adhesion can be controlled and modified by introducing surface functional groups. This is important from a technological point of view. For instance, the wettability of and the adhesion between nonpolar materials are improved when polar groups are grafted onto the surfaces. The increased adhesion in dry air is due to non-dispersion interactions. Such interactions[1] may be dipole–dipole interactions, acid-base interactions, ionic bonds, hydrogen bonds, or covalent bonds. The surface may be modified by blending nonpolar polymers with polar polymers or coupling agents,[2] by chemical treatment,[3,4] by irradiation,[5–7] or by plasma treatment.[8–13] The polar groups and reactive surface sites created by plasma treatment may subsequently be used for further surface modification by grafting of specific functional groups or polymers. Plasma polymerization[8,14–16] may also be used to directly deposit thin polar layers with good adhesion properties.

Plasma technology is becoming a more widely used method due to the following advantages: (i) it is a simple and dry method, (ii) a wide range of polar groups can be introduced onto various substrates, (iii) the reaction is fairly rapid, (iv) the extent of surface modification can be controlled, (v) the degree of modification is rather uniform over the surface, and (vi) the bulk properties of the substrate is not changed significantly.

* To whom correspondence should be addressed.

Journal of Applied Polymer Science, Vol. 41, 1373–1390 (1990)
 CCC 0021-8995/90/7-81373-18$04.00

This paper concerns functionalization of nonpolar polyethylene surfaces and muscovite mica mineral surfaces by plasma polymerization of acrylic acid. The type of functional groups formed under various experimental conditions was determined by means of ESCA and FTIR, and the relationship between the chemical composition and the wettability and the adhesion force was established. Adhesion force, crack formation, delamination, capillary condensation, and compressibility were investigated by means of a surface force apparatus of the type developed by Jacob Israelachvili and coworkers.[17]

EXPERIMENTAL

Materials

Acrylic acid (Merck, purity > 99%) was used as monomer for plasma polymerization. Stabilizer-free, 200-μm thick, PE film (B7518) was obtained from Neste, Finland. It was cleaned ultrasonically for 15 min in a 1 : 1 water/ethanol mixture.

Plasma Polymerization

The design of the plasma reactor is shown in Figure 1. It consists of a large glass vessel (I.D. = 15 cm, length = 65 cm), a double-stage rotary vacuum pump (Leybold Heraeus model D 40 B), a radio frequency (125–375 kHz) power generator (ENI model HPG-2), two external copper electrode bands (3 cm wide, 10 cm apart), a pressure transducer (MKS model 127A), and flow control systems (LH, HI-TEC, and manual controllers). The PE film or mica

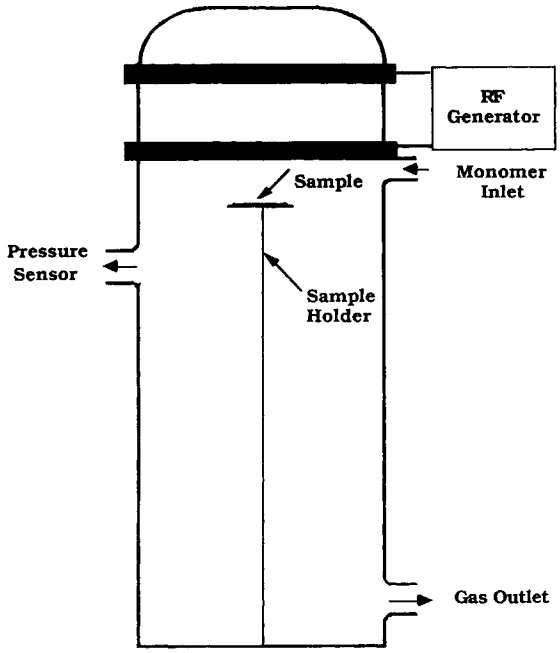

Fig. 1. A schematic diagram of the plasma reactor: I.D., 15 cm; length, 65 cm.

sheet, used as a substrate, was mounted on the top of a stainless steel sample holder. The chamber was evacuated to 5 mtorr before the monomer was introduced from the side of the reaction chamber. The monomer flow rate was 4 standard cubic centimeters per minute (SCCM) and the pressure before ignition of the plasma was 17 mtorr. After plasma polymerization, the chamber was evacuated to 5 mtorr before the sample was removed. The thickness of the deposited layer was estimated with a thickness monitor (INFICON, model XTC) placing an oscillating quartz crystal at the position of the substrate. The plasma polymerized acrylic acid (PPAA) layer was assumed to have a density of 1 g/cm^3 when converting the deposited weight into a layer thickness.

Analysis and Measurement

The chemical composition and the structure of PPAA films were analyzed by means of ESCA (LH 2000) and FTIR/ATR (Nicolet, 5DXB). The chemical composition of PPAA layers deposited under the same conditions did not depend on whether the substrate was mica or PE according to the ESCA C_{1s} spectrum. The oxygen to carbon ratios of PPAA films were calculated from the integrated O_{1s} and C_{1s} peak areas and the atomic sensitivity factors determined by Wagner et al.[18] A KRS-5 crystal was used for attenuated total reflection. The wettability was determined by measuring water contact angles with a goniometer (Rame Hart, model A100).

Delamination, crack formation, capillary condensation, and adhesion force were investigated by means of a surface force apparatus.[17] Two molecularly smooth mica surfaces were first silvered on one side and then glued (silvered side down) onto cylindrical silica discs. The two silvered mica surfaces were mounted in a crossed cylinder configuration inside the surface force apparatus. When white light is directed perpendicular to the surfaces a standing wave pattern (fringes of equal chromatic order) is created. The wavelengths of the standing waves depend on the optical pathlength between the silver layers, and the shape of the fringes reflects the curvature of the surfaces.[17,19] The thickness and the refractive index of the plasma polymer layer were determined by bringing the surfaces into contact and measuring the wavelengths of the standing waves before and after the deposition of PPAA. In a similar way, the surface separation was determined interferometrically to within 0.2 nm. The fringe pattern may also be used to study surface deformation,[20] capillary condensation,[21] and crack formation with a resolution perpendicular and parallel to the surface of about 1 nm and a few μm, respectively. All plasma polymer films appeared to be smooth within this resolution. The surface separation was controlled to within 0.2 nm using a piezo electric tube.

The lower surface is supported by a double variable spring. The deflection of this spring can be determined interferometrically to within 1 nm,[17] which allows the forces acting between the surfaces to be calculated using Hooke's law. According to the Derjaguin approximation,[1,22] the force (F_c) measured in a crossed cylinder configuration normalized by the geometric mean radius (R) is related to the free energy of interaction per unit area for flat surfaces (G_f) by

$$F_c/R = 2\pi G_f \tag{1}$$

RESULTS

Deposition Characteristics

The deposition of a plasma polymer is characterized by the competition between polymer formation and ablation. The deposition rate increases with the discharge power until a saturation value, corresponding to complete monomer activation, is reached.[23] The deposition rate was measured as a function of the discharge power at three different positions in the reactor. The three positions were 10 cm above the monomer inlet (+10 cm), at the monomer inlet (0 cm), and 10 cm below the monomer inlet (−10 cm). At all positions, as shown in Figure 2, the deposition rates reached the maximum values at or below 5 W. As the discharge power increased the deposition rate decreased due to an increased ablation. The decrease was more pronounced at the 10 cm and 0 cm positions (in the electrode band gap) compared to at the −10 cm position (out of the electrode band gap). The reason is that species that can cause ablation, such as high-energy electrons and ions, are concentrated in the electric field between the electrodes.

A sudden reduction of the discharge power from 50 W to 5 W caused the deposition rate to increase by a factor of almost 10 for 2 seconds, and then to decrease gradually to the steady-state value at 5 W. This shows that the number and energy of species that cause ablation are rapidly reduced, whereas the polymerizable species remain active until being deposited on a solid surface. The deposition rate measured immediately after reduction of the discharge power may be a good measure of the polymer formation rate at 50 W.

The ignition of the plasma caused the pressure inside the reactor to increase (Fig. 3), i.e., more molecular fragments and reaction by-products formed than monomers consumed by polymerization. When the plasma is turned off, the pressure initially dropped below the equilibrium value (17 mtorr) and then gradually increased to 17 mtorr. This shows that polymerization continues

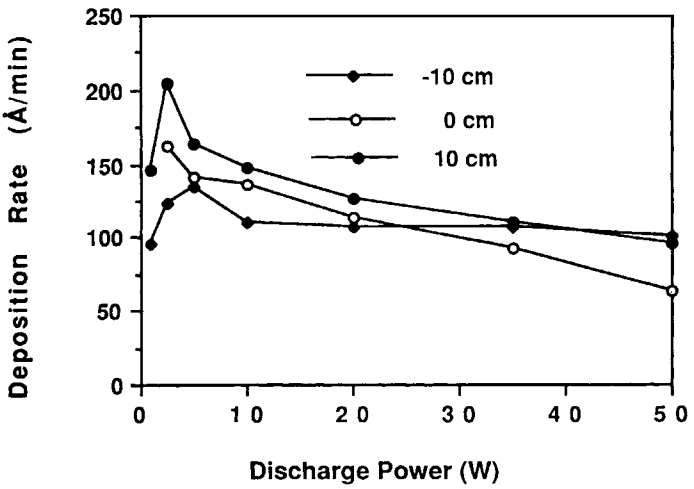

Fig. 2. Deposition rates of plasma polymerized acrylic acid as a function of discharge power: 0 cm refers to the position of monomer inlet; 10 cm and −10 cm refers to the position above and below the monomer inlet, respectively: the monomer flow rate, 4 SCCM.

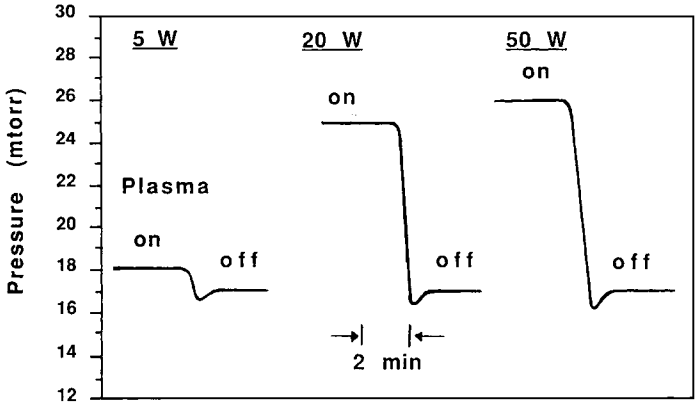

Fig. 3. Pressures before and after plasma polymerization of acrylic acid: monomer flow rate, 4 SCCM.

even after the plasma has been turned off, whereas hardly any new molecular fragments or by-products are formed. The continuing polymerization was confirmed with the thickness monitor.

Chemical Composition and Structure

The FTIR/ATR spectrum of a PPAA film prepared at a discharge power of 5 W (Fig. 4) was very similar to the spectrum of poly(acrylic acid) prepared by conventional polymerization techniques.[24] In particular, the FTIR spectrum shows that the film contains a high density of C(O)OH groups. The main

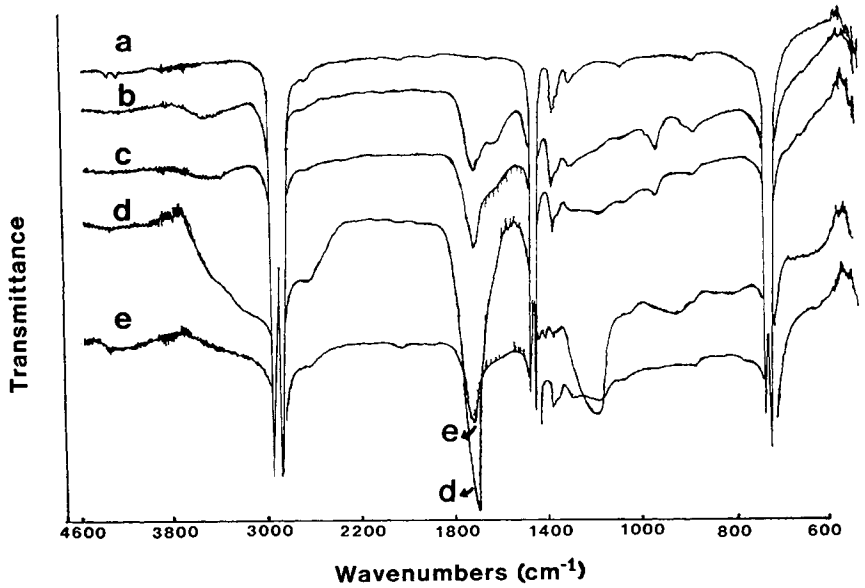

Fig. 4. FTIR/ATR spectra of (a) untreated, (b) plasma polymerized acrylic acid deposited at 50 W, (c) at 20 W, (d) at 5 W, and (e) at 5 W followed by washing in water for 5 min; polyethylenes: thickness of the plasma polymers, approximately 1000 Å.

absorption peaks are: a broad OH stretching absorption band due to monomeric and dimeric C(O)OH between 3637 cm^{-1} and 2376 cm^{-1}; a strong C=O stretching absorption band between 1828 cm^{-1} and 1559 cm^{-1} with the maximum at 1713 cm^{-1}; an absorption peak due to coupled C—O stretching and OH deformation between 1400 cm^{-1} and 1332 cm^{-1}; and a strong C—O stretching absorption peak between 1332 cm^{-1} and 1135 cm^{-1} with the maximum at 1195 cm^{-1}. An absorption band due to C(O)OH dimers appears between 999 cm^{-1} and 875 cm^{-1}. All these peaks are weaker for PPAA films prepared at higher discharge powers (20 W and 50 W). Instead, new peaks (more intense for a film prepared at 50 W compared to a film prepared at 20 W) appear, which demonstrates a structural modification of the acrylic acid during plasma polymerization/deposition. One new peak, possibly due to keto groups conjugated with double bonds, appears as a shoulder at the right side of the C=O stretching absorption peak. Another peak due to —HC=CH— (*trans*) deformation is present at 969 cm^{-1}. The brownish color of PPAA films prepared at 50 W is most likely related to these structures.

Quantitative information about the chemical composition and structure of the outermost (5 nm) surface layer was obtained by means of ESCA. The samples were analyzed after 1-d storage in dry air. The oxygen to carbon ratios were 0.65 for a film prepared at 5 W, 0.40 at 20 W, and 0.32 at 50 W. These values are lower than that of the monomer (0.67). The oxygen deficiency is due to modification of C(O)OH groups during plasma polymerization/deposition. This is demonstrated in Figure 5, where the C_{1s} spectra of PPAA films prepared at 5, 20, and 50 W are displayed. The fractions of oxidized carbon atoms in these films are almost the same as in the pure monomer (0.33). However, the fraction of C(O)O— type carbon atoms is lower than in the monomer and decreases with increasing discharge power.

The C(O)O— type carbon atoms are those of either carboxylic acids or carboxylate esters, and the C—O type carbon atoms are those of alcohols, ethers, or epoxides. If all C(O)O— type carbon atoms are those of acids and all C—O type carbon atoms are those of alcohols, the oxygen to carbon ratio estimated from the deconvoluted C_{1s} signal (2 oxygens/carbon for C(O)O— type carbon atoms and 1 oxygen/carbon for the other type of oxidized carbons assuming no O—C—O type carbon atoms and peroxides) should be the same as the oxygen to carbon ratio estimated from the areas of O_{1s} and C_{1s} signals. This is almost the case for the PPAA film prepared at 5 W, as shown in Table I. However, as the discharge power increases the difference between the two calculations becomes larger, indicating that more ester, ether, and epoxide groups are formed. The obvious interpretation is that the film becomes more crosslinked or branched as the discharge power increases. This is consistent with the observation during adhesion force measurements that the PPAA films prepared at 50 W have a rigid structure whereas the films prepared at 5 W have a soft and tacky structure.

Wettability

The wettability of PPAA films depended on the chemical composition of the surface layer, which was affected by the discharge power and the substrate position in the reactor. The wettability also varied with the storage time and environment.

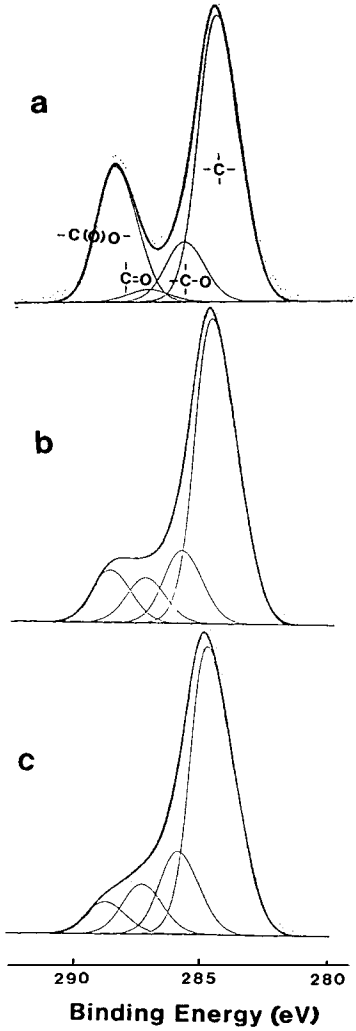

Fig. 5. ESCA C_{1s} spectra of (a) plasma polymerized acrylic acid at 5 W, (b) at 20 W, and (c) at 50 W; samples were analyzed 1 d after the preparation; thickness of the plasma polymers, approximately 300 Å.

How the wettability is affected by the sample position was investigated by placing a PE film (45 × 2.5 cm, contact angle 90°) vertically in the reactor and measuring the contact angle along the film after deposition of PPAA at 5 W for 2.5 min. The contact angle varied from 22° on the part of the film exposed to the intense glow zone (between the electrode bands) to 5° on the part of the film located outside the glow zone, as shown in Figure 6.

Small (5 × 2.5 cm) PE films placed horizontally at the −10 cm position were used to investigate the effect of discharge power on the wettability. The contact angle immediately after plasma polymerization increased with the discharge power, as shown in Table II. This is rationalized by the observation that the polar groups in PPAA films change from highly polar C(O)OH groups to less polar groups such as C=O, C(O)O−C, or C−O when the discharge power increases.

TABLE I
Oxygen to Carbon Ratios in Plasma Polymerized Acrylic Acid at Various Discharge Powers[a]

Discharge power (W)	(O/C)c	(O/C)a	(O/C)c — (O/C)a
5	0.673	0.654	0.019
20	0.431	0.400	0.031
50	0.406	0.320	0.086

[a] (O/C)c and (O/C)a is the oxygen to carbon ratio calculated from the degree of carbon oxidation (determined from the C_{1s} photoelectron peak deconvolution) and from the O_{1s} and C_{1s} peak areas, respectively.

The contact angle increased to between 35 and 63° when PPAA films prepared at 5 W had been stored in water overnight. The lowest contact angle was observed on the part of the film exposed to the intense glow zone (see Fig. 6). The large increase in contact angle could be due to dissolution of highly hydrophilic fragments or molecules (adsorbed monomers or homopolymers not grafted to the surface), configurational change (rotation of hydrophilic groups), or migration of hydrophilic segments. The intensities of the carboxylic acid FTIR/ATR absorption peaks remarkably decrease after immersion in water [see Fig. 4(d)]. Evidently, dissolution of hydrophilic molecules is one of the main reasons for the observed increase in water contact angle. This was supported by the decrease in film thickness observed during adhesion force measurements in water.

The contact angles on PPAA films prepared at 5 W increased during storage in dry and humid air (see Table II). Dissolution of hydrophilic molecules can be ruled out under these conditions, and configurational change or migration in the surface layer has to be responsible for the observed changes in wettability.

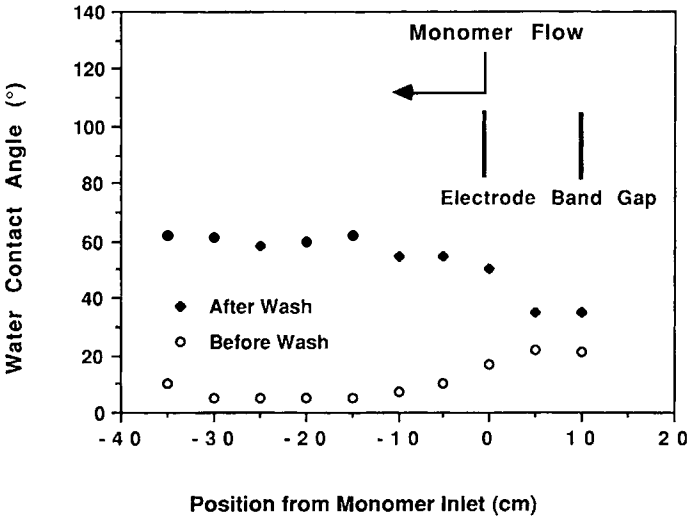

Fig. 6. Advancing water contact angles along a plasma polymerized acrylic acid film deposited onto a polyethylene film before and after overnight washing in water; the film was vertically placed in the reactor; monomer flow rate, 4 SCCM; discharge power, 5 W.

TABLE II
Water Contact Angles on Plasma Polymerized Acrylic Acid Films Deposited on Polyethylene Films

Sample condition	Discharge power (W)		
	5	20	50
Just after deposition	15°	42°	55°
Stored 1 d in dry air	20°	48°	55°
Stored 1 d in 50% RH	[a]	48°	56°
Stored 1 d in 92% RH	55°	48°	61°
Stored 8 d in dry air	43°	—	—
Stored 8 d in 50% RH	40°	—	—
Stored 8 d in 92% RH	63°	—	—
Immersed 5 min in water	53°	48°	55°

[a] The contact angle varied from point to point on the sample ranging between 10 and 43°. The contact angle on an uncoated polyethylene surface was 90°.

The C_{1s} ESCA spectra of PPAA films prepared at 5 W (Fig. 7) show that a large number of C(O)O— type carbon atoms remain in the surface after 8 d storage in dry air [compare Figure 5(a)]. Hence, in dry air hydrophilic groups reorient in the outermost surface to a degree sufficient to affect the wettability but not enough to significantly change the ESCA spectrum (the electron mean free path is 2–5 nm). This implies that configurational rearrangement is the main reason for the observed increase in contact angle. In contrast, the C_{1s} ESCA spectrum changes significantly after the sample is stored in humid air. This shows that extensive migration of polar molecules into the interior of the sample takes place.

Hardly any change in the contact angle of PPAA films prepared at a high discharge power was observed during storage in dry or humid air. This is due to the highly crosslinked structure of these films, which prevents large configurational and migrational changes.

Adhesion Force

Adhesion forces between mica surfaces coated with PPAA or plasma polymerized ethylene (PPE) films were measured with a surface force apparatus.[17] The adhesion force was determined in dry air with a beaker of P_2O_5 in the measuring chamber, in humid air with a beaker of water in the chamber, and in water. The results are summarized in Table III. When the curved surfaces were brought into molecular contact, a strong attractive force deformed the glue holding the mica to the silica disc and flattened the contact region. The flat region in dry air had a diameter of about 60–80 μm. During the separation process, the contact diameter decreases gradually until the surfaces suddenly jump apart. This jump takes place when the bending force of the spring holding the lower surface just exceeds the adhesion force. The pull-off force (F) is determined from the jump distance using Hooke's law. The value of the pull-off force is normalized by the local geometric mean radius of the cylindrical

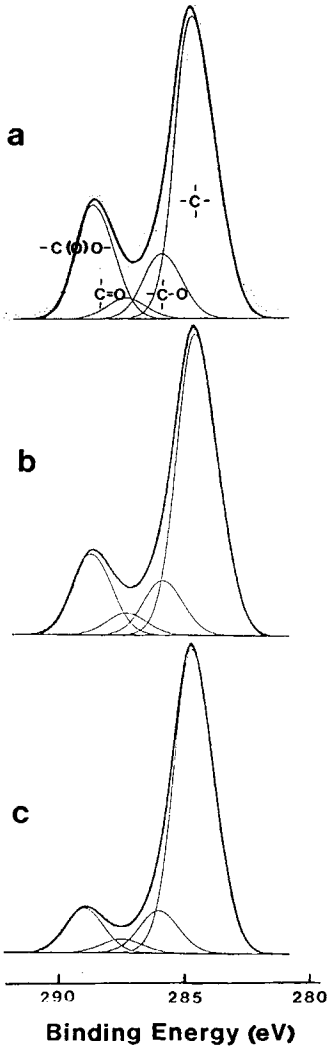

Fig. 7. ESCA C_{1s} spectra of plasma polymerized acrylic acid deposited at 5 W after 8-d storage in (a) dry air, (b) humid air of 50% RH, and (c) humid air of 92% RH; thickness of the plasma polymers, approximately 300 Å.

surfaces (R). For simplicity, the quantity F/R will be referred to as the adhesion force.

The adhesion force between bare mica surfaces in dry air was 630 mN/m. This is in agreement with other values reported in the literature.[21] The adhesion force between PPAA-coated mica surfaces (a 20-nm thick film prepared at 5 W, refractive index 1.51 ± 0.05) in dry air was considerably larger (1200 ± 200 mN/m). The film was locally disrupted, because of strong adhesion, as the surfaces were separated from molecular contact.

In 100% humidity the adhesion force was lowered to 670 mN/m, and the thickness of the layer could be decreased (about 1–2 nm) when a strong external force was applied. A large capillary condensate formed around the contact region. It covered a circular area with a diameter of about 200 μm and bridged a 200-

TABLE III
Pull-off Force Normalized by the Geometric Mean Radius

Surfaces	Environment	Adhesion force (mN/m)
PPAA 5 W/PPAA 5 W	Dry air	1200
	100% Humidity	670
	Water	0
PPAA 50 W/PPAA 50 W	Dry air	200
	100% Humidity	490
PPAA 5 W/Ethylene	Dry air	320
	100% Humidity	260
Ethylene/Ethylene	Dry air	70

nm gap between the surfaces. The adhesion force has, in this case, three contributions: a contribution from the molecular forces acting between the PPAA films across water, a Laplace pressure contribution, and a contribution from the surface tension of water around the capillary perimeter (for a detailed discussion the reader is referred to the paper by Christenson[20]).

No adhesion was observed between PPAA-coated mica surfaces (prepared at a discharge power of 5 W) in water. Instead, a long-range repulsive force was measured. The force observed after 1-h immersion in water is shown in Figure 8. A double-layer force dominates the interaction at large distances (more than 60 nm out from bare mica contact at D=O). The Debye length was about 120 nm, corresponding to a monovalent electrolyte concentration of 6×10^{-6} M. At separations below 60 nm a repulsive steric force due to compression of the PPAA layer was observed. Clearly, the layer swells considerably in water. Despite the extensive swelling the thickness of the compressed layer

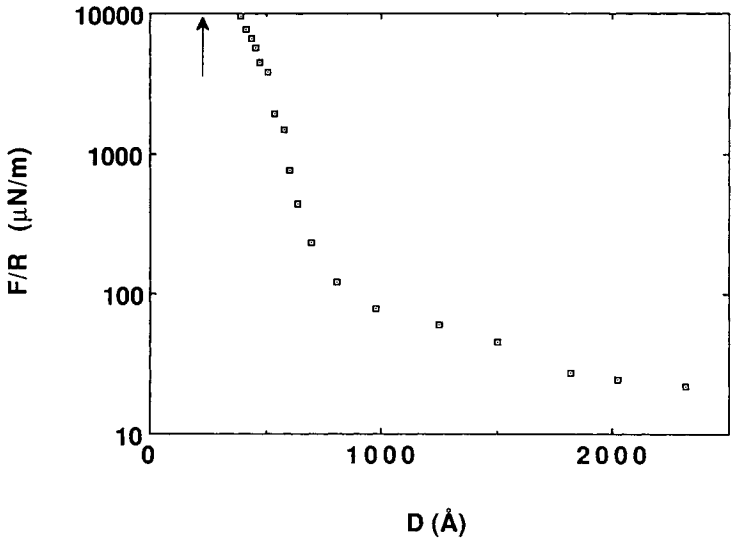

Fig. 8. The force normalized by the radius as a function of distance between plasma polymerized acrylic acid (5 W) deposited mica surfaces in water; a strong repulsive force due to steric repulsion is present at distance below 600 Å; the thickness of the layer under a high load (0.1 N/m) is indicated by the arrow.

was less in water than in dry air (10 nm on each surface compared to 20 nm). The decrease of the compressed layer thickness is due to both dissolution of homopolymers and a pressure-induced surface diffusion of polymers from the contact zone. The refractive index of the compressed layer was the same in water and dry air.

The adhesion force between a PPAA film prepared at 5 W and a nonpolar PPE film (10 W, 10 SCCM, 2 min; water contact angle 87°) was 320 mN/m in dry air and 260 mN/m in 100% humidity. The adhesion force in dry air was considerably larger than the adhesion force between two PPE surfaces (70 mN/m). The low adhesion in humid air is surprising considering that a capillary condensate did form around the contact zone. The explanation is that the separation was largely due to cohesive failure in both the PPE film and the PPAA film instead of adhesive failure between the PPAA and the PPE film. After separation it was observed that cracks had formed in the PPE film and that material had been transferred from the PPAA film to the PPE film.

The adhesion force between PPAA films decreased with increasing discharge power. The adhesion between two 50-nm thick films prepared at 50 W was 200 mN/m in dry air and 490 mN/m in 100% humidity. In humid air a comparatively small capillary condensate with a diameter of 100 μm and a thickness of 20 nm formed around the contact region. The refractive index of the PPAA film prepared at 50 W was 2.0.

Deformation and Disruption

When two mica surfaces coated with a PPAA film prepared at 50 W were squeezed together by an external force no change in film thickness was observed. This indicates that the film is rigid, which is consistent with the high degree of crosslinking and branching deduced from FTIR and ESCA analyses. In dry air, the PPAA film remained intact when the surfaces were brought into adhesive contact and then separated. However, in humid air cracks formed in the film during the separation process. The cracks appeared mainly in the region covered with capillary condensate. From the shape of the fringe pattern the size of the cracks were estimated to be about 5 μm wide with edges protruding 20–30 nm from the surface. The refractive index of the protruding part was only 1.2, showing that the protrusion is not homogeneous but contains many voids. Clearly, water molecules lower the internal cohesion and facilitate the formation of cracks. However, the film thickness was unaffected by the humidity showing that not very many water molecules penetrated the film. The bond between the mica surface and the PPAA film was broken when the surfaces were immersed in water. Hence, under this condition, delamination from the mica surface was observed.

PPAA films prepared at 5 W had quite different properties. When a strong external force was applied, a 20-nm thick film could be compressed about 0.5 nm in dry air and about 1–2 nm in humid air. In water, an even more extensive compression was possible. (Note that the decrease in film thickness observed in water and humid air is partly due to the surface diffusion of polymers from the contact zone.) The films were damaged when separated from adhesive contact in both dry and humid air. No cracks were formed but the surface became rough due to cohesive failure within the films or adhesive failure between the mica and the film. An electron micrograph of the damaged film is shown in

Figure 9. Tiny pits and lumps are shown on the microscopically smooth film, indicating that materials are transferred from one surface to the other during the separation.

DISCUSSION

Polymerization Mechanism

In a plasma, acrylic acid monomers may polymerize by opening of the double bond or by formation of reactive species through fragmentation. Opening of a C=C bond requires less energy, 2.74 eV, than dissociation of a C—C bond, for instance, which requires 3.61 eV. Hence, at a low discharge power the polymerization mainly proceeds by opening of double bonds. However, note that the polymerization mechanism is not a chain-growth mechanism as in conventional polymerization of acrylic acid.[23] The energy transferred to monomer molecules (primarily by inelastic electron impact) increases as the discharge power increases and polymerization by fragmentation becomes more important. Furthermore, at a high discharge power, the deposited layer is bombarded by energetic species, resulting in structural modification and ablation. The small pressure increase observed during plasma polymerization at 5 W (from 17 to 18 mtorr) and the larger pressure increases observed at 20 and 50 W (to 25 and 26 mtorr, respectively) indicate that the degree of fragmentation increases with increasing discharge power. Accordingly, a soft linear PPAA polymer is formed at 5 W, whereas a highly branched or crosslinked polymer is formed at

Fig. 9. A scanning electron microscope (SEM) picture of a plasma polymerized acrylic acid layer (5 W) after separation from molecular contact during adhesion force measurement; the picture shows tiny lumps and pits indicating material transfer during separation.

50 W. Fragmentation and ablation processes are responsible for the alteration of C(O)OH groups observed with FTIR/ATR and ESCA and the reduction in wettability.

Wettability

Polymers have a high rotational and migrational mobility[25,26] unless they are crosslinked or form crystals. Hence, they may rearrange in response to a changed environment. In air, hydrophobic groups and molecules tend to orient or move towards the surface to reduce the interfacial energy. For the same reason, hydrophilic groups and molecules are concentrated at the surface in water. Keeping this in mind, the contact angle increase on the PPAA film prepared at 5 W stored in dry air is easy to understand. However, the even larger increase observed for samples stored in humid air is unexpected. We postulate that this is due to hydrogel formation.

The PPAA film prepared at 5 W can form a hydrogel structure through crosslinking by hydrogen bonds. Water contact angles on hydrogels in air are surprisingly high when the hydrogel contains water.[27] The general explanation is that hydrophilic groups reorient toward the interior of the hydrogel, which contains a pool of water. These water molecules will also decrease the number of polymer–polymer hydrogen bonds and cause an increase in the mobility of hydrophilic groups and segments. This may lead to an increase in the contact angle with increasing water content of the hydrogel as observed for PPAA films prepared at 5 W. While the samples are dried in a vacuum ESCA chamber the water concentration is higher in the bulk polymer than on the surface. Thus, hydrophilic groups, especially C(O)OH groups, hide in the bulk, and a lower number of hydrophilic groups are located on the surface compared to the situation in water.

Adhesion Forces in Dry Air

The interaction between uncharged nonpolar surfaces in dry air is determined by dispersion forces. The nonretarded van der Waals force between crossed cylinders is given by

$$F_c/R = A/6D^2 \tag{2}$$

where A is the nonretarded Hamaker constant. For most nonmetals interacting across air the Hamaker constant is of the order of $3\text{–}10 \times 10^{-20}$ (J).[1] For instance, for hydrocarbon and mica interacting across air the Hamaker constant is 5×10^{-20} and 10×10^{-20} (J), respectively. When calculating the van der Waals contribution to the surface energy and the adhesion force it is common to use a closest approach distance of 0.165 nm.[1] Hence, the van der Waals contribution to the adhesion force in dry air between smooth crossed cylinders is expected to be approximately 300 mN/m for hydrocarbons and 600 mN/m for mica. The adhesion force in air between mica surfaces rendered nonpolar by deposition of a 2-nm thick Langmuir–Blodgett layer of dimethyldioctadecylammonium bromide has been measured to be 310 mN/m, which is in good agreement with the calculated value considering only dispersion forces. In contrast, the adhesion forces between PPE films (70 mN/m) and between PPAA films prepared at 50 W (200 mN/m) are lower than the expected adhesion

force caused by dispersion interactions. This shows that the surfaces are rough on a level that cannot be detected by the interferometric technique. It is not clear whether the higher adhesion force between PPAA films prepared at 50 W compared to PPE films is due to better smoothness or due to contributions from nondispersion forces.

It is interesting that the adhesion force measured between a PPAA film prepared at 5 W and a PPE film (320 mN/m) is roughly as expected when only dispersion forces are operating between smooth surfaces. It is likely that the soft and flexible PPAA film deforms to match the shape of the rough and rigid PPE film. Such a flexibility should be of great importance from a technical point of view considering that molecularly smooth surfaces are never found in practical systems.

The very large adhesion force observed between PPAA films prepared at 5 W (1200 mN/m, which is almost four times higher than the adhesion force expected from dispersion interactions only) shows that nondispersion interactions and/or chain entanglement contribute to the adhesion force. The ESCA and FTIR/ATR analyses show that chemical groups with hydrogen bonding abilities are present on the surface, and it is likely that such bonds contribute to the adhesion force.

The adhesion force between curved surfaces is related to the surface tension, γ. For smooth nondeformable surfaces in a crossed cylinder configuration (and for a sphere against a flat surface) Derjaguin[28] derived the relationship

$$F_c/R = 4\pi\gamma \tag{3}$$

According to the theory of Johnson, Kendall, and Roberts (JKR theory)[29] the adhesion force and surface tension for deformable surfaces are related by

$$F_c/R = 3\pi\gamma \tag{4}$$

The surfaces in our system are deformable and a large flat region appears when the surfaces are brought into molecular contact. Hence, one would expect eq. (4) to describe the present situation better than eq. (3). Notice, however, that experiments by Israelachvili et al.[19,30] have shown that for nonplastic surfaces the decrease in contact diameter prior to the jump is in agreement with the JKR theory, whereas the adhesion force appears to have a value in between those predicted by eqs. (3) and (4).

Capillary Condensation and Adhesion

The influence of capillary condensation on the adhesion between smooth nondeformable solid surfaces has been investigated in detail by Christenson.[20] The detailed analysis given in ref. 20 will not be recapitulated here but the main points will be discussed. When the contact angle of the liquid is low the main contribution to the adhesion force arises from the Laplace pressure difference over the curved interface, which is given by

$$F_{\text{Lap}}/R = 4\pi\gamma_L \cos\theta \tag{5}$$

where γ_L is the surface tension of the liquid and θ the contact angle. There is also a contribution from the direct solid–solid interaction across water given by

$$F_{SS}/R = 4\pi(\gamma_{SL} - \gamma_{SS}^{L}) \tag{6}$$

where γ_{SL} is the interfacial tension between the liquid and the solid and γ_{SS}^{L} the interfacial tension between the two solids in liquid environment. This latter term is zero for perfect surfaces, but due to imperfections at the solid–solid contact it is important for real surfaces. A third contribution from the surface tension around the circumference is negligible when the contact angle is low. Accordingly, the total adhesion force in the presence of the capillary is

$$F/R = 4\pi(\gamma_L \cos\theta + \gamma_{SL} - \gamma_{SS}^{L}) = 4\pi(\gamma_{SV} - \gamma_{SS}^{L}) \tag{7}$$

where γ_{SV} is the interfacial tension between the solid and the vapor. The last equality arises from the Young equation. By comparison, the adhesion in dry air is given by

$$F/R = 4\pi(\gamma_S - \gamma_{SS}) \tag{8}$$

where γ_S is the interfacial tension between the solid and dry air and γ_{SS} the interfacial tension between the two solids in dry air. Adsorption of water vapor lowers the interfacial tension and γ_{SV} is normally lower than γ_S. If we assume that the solid–solid interfacial tension is not affected by the humidity, the adhesion force decreases with increasing humidity. This is observed for PPAA films prepared at 5 W (the adhesion force decreases from 1200 mN/m in dry air to 670 mN/m in 100% humidity). The adhesion force expected in humid air according to eq. (7) (assuming that γ_{SL} is zero, $\gamma_{SS}^{L} = \gamma_{SS}$ and $\theta = 15°$) is 870 mN/m. This is 30% larger than the observed value.

The adhesion between rough surfaces increases when capillary condensation takes place.[1] The reason is that the adhesion in dry air is low due to a small effective contact area (a large γ_{SS}). In the presence of a capillary the adhesion force for low-contact angles is to a good approximation given by eq. (5). Based on this equation the adhesion force between PPAA films prepared at 50 W is expected to be 520 mN/m, which is in good agreement with the measured value (490 mN/m).

Deformation and Tacticity

The JKR theory[29] considers the behavior of deformable solids in contact. Under the action of attractive molecular forces a flat contact region (with diameter d) is created. One prediction of the JKR theory is that during separation the contact diameter should decrease to 0.63 d before the surfaces jump apart.

In our experiments the surfaces were deformable and the contact diameter decreased during the separation process. The decrease of the contact diameter prior to the jump was roughly in agreement with the prediction of the JKR theory except for PPAA films prepared at 5 W. For such films the contact diameter decreased to less than 0.2 d before the surfaces jumped apart. This shows that such films are deformable and tend to stick together like a glue. It

is likely that linear polymers from the opposing surfaces gets entangled in the contact region. This would also rationalize the large adhesion force and the cohesive failure in the PPAA film prepared at 5 W.

Water and Crack Formation

The JKR theory predicts that when deformable surfaces are in adhesive contact there is a tensile stress near the periphery of the contact region and a compressive stress near the center.[20,29] Hence, the surfaces are under the greatest mechanical stress close to the rim of the flat contact region, and it is expected that the surfaces are most easily damaged in this region. This was also observed for PPAA films prepared at 50 W.

The presence of water often reduces the adhesion in various laminates and other products. One reason for this effect is that water absorption reduces the cohesion in hydrophilic films and the adhesion to a hydrophilic substrate. This is due to the fact that water solvates polar groups and whereby lowers the interfacial tension. Water molecules may also break hydrogen and ionic bonds and even hydrolyze some covalent bonds. These effects combine to make crack formation easier in humid air than in dry air. This was clearly observed for PPAA films prepared at 50 W. In humid air many cracks formed around the contact zone in the area covered with capillary condensate. The large mechanical stress combined with the lowered cohesion of the film due to the presence of water disrupts the film. Note that the mechanical stress alone is not sufficient for disrupting the film (no cracks were formed in dry air). Water that penetrates between a hydrophilic surface and a coating may cause delamination. This was observed for PPAA films (50 W) on mica substrates after immersion in water.

CONCLUSIONS

Deposition of PPAA onto nonpolar surfaces makes the surfaces hydrophilic. The hydrophilicity increases as the discharge power decreases. The reason is that C(O)OH groups are converted to less polar C=O, C(O)O−C, and C−O groups at higher discharge powers. The wettability of PPAA films is affected by the environment due to reorientation of mobile, hydrophilic groups or segments. This is clearly seen for the more linear and mobile films prepared at 5 W. The more crosslinked films prepared at 50 W are less sensitive to environmental changes.

PPAA films prepared at 5 W are soft and contain a large number of carboxylic acid groups. The adhesion force between such films is high due to hydrogen bonds and/or chain entanglement. The adhesion force decreases when the humidity is increased. This is caused by absorbed water molecules lowering the interfacial tension. PPAA films prepared at 50 W are harder and have a comparatively low density of carboxylic groups capable of forming hydrogen bonds. Due to surface roughness and the lack of hydrogen bond interactions the adhesion force between such films is low. When these films are compressed cracks are easily formed in humid air (but not in dry air).

The surface force apparatus developed by Israelachvili and coworkers has proved to be an excellent tool for the study of adhesion forces and mechanical properties of plasma polymerized films.

References

1. J. N. Israelachvili, *Intermolecular and Surface Forces with Applications to Colloidal and Biological Systems,* Academic Press, London, 1985.

2. E. P. Plueddemann, in *Surface and Colloid Science in Computer Technology,* K. L. Mittal, Ed., Plenum Press, New York, 1987, pp. 143–153.

3. E. Kiss, C. G. Gölander, and J. C. Ericksson, *Progr. Coll. & Polymer. Sci.,* **74,** 113 (1987).

4. T. S. Keller, A. S. Hoffman, B. D. Ratner, and B. J. McElroy, in *Physicochemical Aspects of Polymer Surfaces,* K. L. Mittal, Ed., Plenum Press, New York, 1983, Vol. 2, pp. 861–879.

5. H. L. Needle, *J. Appl. Polym. Sci.,* **15,** 2559 (1971).

6. L. Williams and V. Stannett, *Text. Res. J.,* **38,** 1056 (1968).

7. M. Suzuki, T. Tamada, H. Iwata, and Y. Ikada, in *Physicochemical Aspects of Polymer Surfaces,* K. L. Mittal, Ed., Plenum Press, New York, 1983, Vol. 2, pp. 923–941.

8. H. V. Boenig, *Fundamentals of Plasma Chemistry and Technology,* Technomic, Lancaster, 1988.

9. P. W. Rose and E. M. Liston, *Plastic Eng.,* 40 (October 1985).

10. M. Hudis, in *Techniques and Applications of Plasma Chemistry,* J. R. Hollahan and A. T. Bell, Eds., John Wiley, New York, 1974, pp. 113–145.

11. T. Ohmichi, H. Tamaki, H. Kawasaki, and S. Tatsuta, in *Physicochemical Aspects of Polymer Surfaces,* K. L. Mittal, Ed., Plenum Press, New York, 1983, Vol. 2, pp. 793–800.

12. J. R. Hollahan and B. B. Stafford, *J. Appl. Polym. Sci.,* **13,** 807 (1969).

13. M. Suzuki, A. Kishida, H. Iwata, and Y. Ikada, *Macromolecules,* **19,** 1804 (1986).

14. D. H. Kaelble, *Physics and Chemistry of Adhesion,* John Wiley, New York, 1971.

15. A. Bradley and J. D. Fales, *Chem. Tech.,* 232 (1971).

16. A. Moshonov and Y. Avny, *J. Appl. Polym. Sci.,* **25,** 771 (1980).

17. J. N. Israelachvili and G. E. Adams, *J. Chem. Soc. Faraday Trans. I,* **74,** 975 (1978).

18. J. N. Israelachvili, *J. Colloid Interface Sci.,* **44,** 259 (1973).

19. R. G. Horn, J. N. Israelachvili, and F. Pribac, *J. Colloid Interface Sci.,* **115,** 480 (1987).

20. H. Christenson, *J. Colloid Interface Sci.,* **121,** 170 (1988).

21. B. V. Derjaguin, *Kolloid Zeits.,* **69,** 155 (1934).

22. H. Yasuda, *Plasma Polymerization,* Academic Press, London, 1985.

23. C. J. Pouchert, *The Aldrich Library of FT-IR Spectra, Edition 1,* Aldrich Chemical Company, Milwaukee, WI, 1985, Vol. 2, p. 1182.

24. C. D. Wagner, L. E. Davies, M. V. Zeller, J. A. Taylor, R. H. Raymond, and L. H. Gale, *Surf. Interface Anal.,* **3,** 211 (1981).

25. F. J. Holly and M. J. Owen, in *Physicochemical Aspects of Polymer Surfaces,* K. L. Mittal, Ed., Plenum Press, New York, 1983, Vol. 2, pp. 625–636.

26. J. D. Andrad, D. E. Gregonis, and L. M. Smith, in *Physicochemical Aspects of Polymer Surfaces,* K. L. Mittal, Ed., Plenum Press, New York, 1983, Vol. 2, pp. 911–922.

27. F. J. Holly and M. F. Refojo, in *Hydrogels for Medical and Related Applications,* J. D. Andrad, Ed., ACS Symposium Series No. 31, ACS, Washington DC, 1976, p. 252.

28. B. V. Derjaguin, V. M. Müller, and Yu. P. Toporov, *J. Colloid Interface Sci.,* **53,** 314 (1975).

29. K. L. Johnson, K. Kendall, and A. D. Roberts, *Proc. Roy. Soc. London A* **324,** 301 (1971).

30. J. N. Israelachvili, E. Perez, and R. K. Tandon, *J. Colloid Interface Sci.,* **78,** 260 (1980).

Received June 6, 1989
Accepted September 25, 1989